0026-895X/91/020289-10$03.00/0

MOLECULAR PHARMACOLOGY, 40:289–298

Ifenprodil Blocks *N*-Methyl-D-aspartate Receptors by a Two-Component Mechanism

PASCAL LEGENDRE[1] and GARY L. WESTBROOK

Vollum Institute and Department of Neurology, Oregon Health Sciences University, Portland, Oregon 97201

Received February 20, 1991; Accepted May 7, 1991

SUMMARY

The inhibition of *N*-methyl-D-aspartate (NMDA) receptor channels by the vasodilatory and anti-ischemic agent ifenprodil was examined on cultured rat hippocampal neurons. Whole-cell and single-channel patch recordings were used. Ifenprodil inhibition of NMDA currents could be separated into two components, with IC_{50} values of 0.75 and 161 μM. The high and low affinity components were both voltage independent but could be separated by their kinetics and dependence on extracellular calcium and glycine. The maximal inhibition of inward current by ifenprodil (≈90%) was equally divided between the two components in 0.3 mM extracellular calcium and 500 nM glycine. The low affinity action of ifenprodil had rapid kinetics and appeared to result from allosteric inhibition of the glycine modulatory site on the NMDA receptor. The macroscopic kinetics of the high affinity component were slow. The rate of onset was concentration dependent, and complete recovery required 1–2 min. Unlike open-channel blockers, ifenprodil block was not use dependent, and pre-exposure to ifenprodil also reduced subsequent NMDA responses. Low concentrations of ifenprodil were less effective after calcium-dependent inactivation of whole-cell currents, but the IC_{50} was unaffected, suggesting that calcium and ifenprodil act on a common set of channels. On outside-out membrane patches, ifenprodil reduced the frequency of channel opening without altering the single-channel conductance. Open time histograms of the large conductance events revealed two mean open times of ≈2 and 8 msec, but only the duration of the long openings was decreased by ifenprodil. This effect was concentration dependent and revealed a blocking rate constant of 6×10^7 $M^{-1}sec^{-1}$. However, the proportion of current blocked by low concentrations of ifenprodil was larger in outside-out patches than in whole-cell recordings, suggesting that intracellular factors may influence ifenprodil efficacy. These results indicate that high affinity ifenprodil binding is extracellular and does not require agonist binding or channel opening. Because low concentrations of ifenprodil only partially inhibited the current and affected only the long openings, ifenprodil may promote a modal shift in channel gating.

The use of glutamate receptor antagonists as 'neuroprotective' agents in hypoxic-ischemic brain damage has been actively studied in the past few years (1, 2). Several lines of evidence have suggested that NMDA receptors play an important role in the accompanying neuronal death (reviewed in Ref. 3). Calcium influx through NMDA channels appears to initiate this process, and NMDA-induced neuronal cell death *in vitro* is dependent on extracellular calcium (4, 5). Thus, potent and selective receptor antagonists for this receptor could be important therapeutic agents. A number of binding sites have been pharmacologically characterized on the NMDA receptor channel (reviewed in Ref. 6). Antagonists act via several of these sites, including the glutamate recognition site, the strychnine-insensitive glycine modulatory site within the NMDA channel, and allosteric sites on the receptor. Although some noncompetitive antagonists such as MK-801 are highly potent, behavioral side effects could become important limiting factors in therapeutic trials (7); thus, it is worthwhile to investigate other compounds with distinct mechanisms of action.

The phenylethanolamine ifenprodil was originally developed as a vasodilator (8) and has been used sporadically as a cerebral vasodilator (e.g., Ref. 9). It has also been reported to have neuroprotective action in animal models of focal cerebral ischemia (10). Recently, ifenprodil has been shown to noncompetitively antagonize NMDA receptors in several experimental preparations (11), but its mechanism of action remains unclear. Ifenprodil is structurally unrelated to other NMDA receptor antagonists and has not been reported to have behavioral side effects. It has been suggested that ifenprodil antagonizes NMDA receptors by an interaction with polyamines (12, 13), which have been reported as positive modulators of NMDA receptor function (14–16). However, other investigators have

This work was supported by United States Public Health Service Grants NS 26494 and MH 46613 and by the McKnight Foundation (G.L.W.). P.L. was supported by NATO Foundation and INSERM.

[1]Present address: Institut Pasteur, Departement des Biotechnologies, INSERM U.261, 75724 Paris Cedex 15, France.

ABBREVIATIONS: NMDA, *N*-methyl-D-aspartate; MK-801, (+)-5-methyl-10,11-dihydro-5*H*-dibenzo[*a*,*d*]cyclohepten-5,10-imine; HEPES, *N*-(2-hydroxyethyl)piperazine-*N*′-(2-ethanesulfonic acid); EGTA, ethylene glycol bis(β-aminoethyl ether)-*N*,*N*,*N*′,*N*′-tetraacetic acid; TCP, *N*-(1-[2-thienyl] cyclohexyl)piperidine; AMPA, α-amino-3-hydroxy-5-methyl-4-isoxazolepropionic acid; DET, diethylenetriamine.

proposed that ifenprodil stabilizes an inactivated form of the channel (17).

We examined the action of ifenprodil on NMDA receptors on hippocampal neurons in cell culture, using whole-cell and single-channel recording. Ifenprodil antagonism of NMDA-activated whole-cell currents had two components, which differed in their mechanism. At high concentrations ifenprodil was a glycine antagonist, but this mechanism of action is unlikely to be significant in the presence of physiological concentrations of glycine. The high affinity component had slow macroscopic kinetics, accounted for 30–50% of the total inhibition, and was not additive with calcium-dependent inactivation of the NMDA channel. The action of ifenprodil could not be attributed to antagonism of polyamines.

Materials and Methods

Cell culture. Cultures of hippocampal neurons were prepared as previously described (18). Hippocampi from postnatal day 1 Sprague Dawley rat pups were incubated in low-calcium saline with papain (5–20 units/ml; Worthington Biochemicals) for 1 hr. The papain was inactivated with bovine serum albumin and trypsin inhibitor, and the tissue was mechanically dissociated and plated onto a confluent layer of hippocampal astrocytes. The culture medium contained minimum essential medium, 0.6% glucose, 5% heat-inactivated horse serum (Hyclone), and a supplement including 200 μg/ml transferrin, 200 μM putrescine, 60 nM sodium selenite, 40 nM progesterone, 40 ng/ml corticosterone, 20 ng/ml triiodothyronine, and 10 μg/ml insulin. Cultures were treated 1 day after plating with a mixture of 5′-fluoro-2-deoxyuridine and uridine (15 and 35 μg/ml, respectively) to suppress overgrowth of background cells; half-changes of medium were done twice weekly.

Electrophysiology and drug delivery. Standard outside-out and whole-cell patch-clamp recordings (19) were performed on neurons after 1–2 weeks in culture. The extracellular solution contained (in mM) Na, 162; K, 2.4; Ca^{2+}, 1.3 or 0.3; Mg^{2+}, 0; Cl, 167; HEPES, 10; and glucose, 10; pH adjusted to 7.3; osmolarity adjusted to 325 mOsM with sucrose. Tetrodotoxin (500 nM), strychnine (2 μM), and picrotoxin (50 μM) were added to block spontaneous electrical activity and glycine and γ-aminobutyric acid channels, respectively. Patch pipettes were pulled from borosilicate glass (TWF 150, WPI), coated with Sylgard, and fire-polished and had DC resistances of 2–10 MΩ. Pipette solutions contained (in mM) CsCl, 126; CsFl, 14; EGTA, 10; and HEPES, 10; pH adjusted to 7.2 with CsOH; osmolarity adjusted to 295 mOsM. The chamber was continuously perfused (1–2 ml/min) at room temperature (≈20°). Single-channel currents in the outside-out patch configuration and whole-cell currents were recorded using an Axopatch 1B (Axon Instruments), with the current filtered at 10 kHz. Membrane current records were monitored on a chart recorder and stored on videotape for later analysis using a digital data recorder (VR10; Instrutech Corp.).

NMDA (2–10 μM) and ifenprodil (0.3–1000 μM) were dissolved in the extracellular solution and applied via an array of flow pipes (400-μm i.d.) positioned within 100–200 μm of the cell. Each flow pipe was controlled by solenoid valves; solutions were changed by simultaneously closing one valve and opening another. The solution exchange time constant was less than 20 msec, as measured by the change in membrane current evoked by kainic acid in two concentrations of sodium (20). Ifenprodil solutions were freshly prepared before each experiment. Ultrapure calcium and sodium salts (Aldrich) were used in the flow pipes for drug delivery. In most cases, the extracellular glycine concentration was 500 nM; in some experiments, this was varied from 0 to 100 μM; the estimated glycine concentration in nominally glycine-free solutions was 50 nM. Concentration-response curves were fitted with equations given in the figure legends. NMDA was obtained from Cambridge Research Biochemicals; other chemicals were obtained from Sigma.

Single-channel analysis. Low concentrations of NMDA (2 μM) and glycine (500 nM) were used during single-channel recordings, to minimize the number of overlapping events. Single-channel currents were replayed, filtered at 2 kHz (eight-pole Bessel; Frequency Devices), digitized at 10 kHz, and analyzed on an IBM AT-compatible computer using pClamp software (version 5.5). Opening and closing transitions were detected using a 50% threshold criterion. Events briefer than 200 μsec were deleted from the events list when the filter cut-off frequency was 2 kHz. Mean open time histograms were fitted with the sum of two or three exponentials. Amplitude histograms were fitted with the sum of one or more gaussian functions, using least-square methods. Single-channel conductance was checked for each patch, using the observed reversal potential. Cumulative point-per-point amplitude histograms were used to obtain estimates of channel opening probability. Because multichannel patches were used, the estimate of opening probability (P_o) obtained was np, where n is the number of channels and p is the probability of opening for a single channel. Results are presented as mean values ± standard deviation.

Results

Ifenprodil selectively blocks NMDA receptors in a voltage-independent manner. Whole-cell recordings were made from hippocampal neurons after 6–14 days in culture. Neurons were initially voltage-clamped at −50 mV, and drug applications were made by switching between large-bore flow pipes containing either the control medium or test solutions. Fast applications (exchange rate, <20 msec) of NMDA, kainate, or AMPA produced inward currents with fast-on, fast-off macroscopic kinetics in all neurons tested ($n > 100$). To minimize calcium-dependent desensitization of the NMDA-evoked current (21, 22), NMDA was applied in the presence of 0.3 mM $CaCl_2$. As shown in Fig. 1A, a high concentration of ifenprodil (100 μM) applied during the continuous perfusion with NMDA rapidly antagonized the inward current (Fig. 1A). However, the recovery after the application of ifenprodil had two easily separable components, one that was similar to the rate of solution exchange and a second component with a strikingly slower recovery rate. The degree of inhibition as well as the onset and recovery rates were similar at holding potentials of −50 mV and +40 mV. Ifenprodil decreased the NMDA-evoked current at −50 mV to 30 ± 4.6% of control ($n = 16$), compared with 36.2 ± 3.9% ($n = 11$) at +40 mV.

Responses evoked by AMPA showed fast desensitization to a steady state current, whereas kainate responses did not show appreciable desensitization (23). Ifenprodil was applied after the currents had reached a stable level. Ifenprodil had no significant effect on responses evoked by kainate (100 μM) or AMPA (50 μM). In the presence of ifenprodil, the response to kainate was 92 ± 3.7% of control ($n = 10$), whereas the steady state AMPA-evoked response was 104 ± 6.7% ($n = 10$) (Fig. 1B).

Ifenprodil concentration-response curves are biphasic. The dose dependence of ifenprodil action (0.1–300 μM) was tested by application of three different concentrations of ifenprodil to each neuron; the results were then pooled to construct a concentration-response curve. All neurons were tested with NMDA (10 μM) at a holding potential of −50 mV. The inhibition by 3 and 100 μM ifenprodil for one neuron is shown in Fig. 2A. Because the rate of onset of antagonism was concentration dependent, the duration of application was adjusted to allow the current to reach steady state levels. Ifenprodil had no effect at concentrations lower than 0.1–0.3 μM, and the maximal inhibition was observed at 300 μM (15 ± 3.8% of control, $n = 4$). Although inhibition was not complete at 300

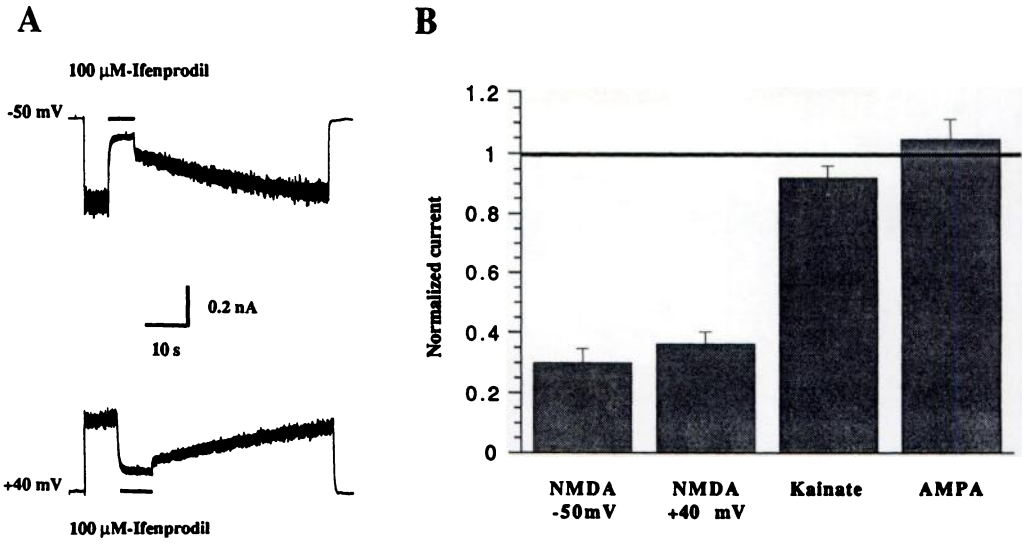

Fig. 1. A, The inward current evoked by flow pipe application of 10 μM NMDA was blocked by a 10-sec coapplication of ifenprodil (100 μM) at holding potentials of −50 and +40 mV. Note the slow recovery after removal of ifenprodil. B, In the presence of ifenprodil (100 μM), the NMDA-evoked current was reduced to 30% of control at −50 mV, whereas responses evoked by kainate (100 μM; V_h, −50 mV) and AMPA (50 μM; V_h −50 mV) were not significantly altered. The extracellular solution for this and subsequent figures contained 0.3 mM Ca^{2+} and 500 nM glycine, unless otherwise noted.

μM, the limited solubility of ifenprodil at ≥1 mM prevented testing of higher concentrations. The normalized inhibition curve was biphasic and was fitted with the sum of two binding site isotherms of the form

$$I_{IFL} = I_{CON}\{A_1(1 - ([IFL]/([IFL] + IC_{50_1}))) + A_2(1 - ([ILF]/([IFL] + IC_{50_2})))\}$$

where I_{CON} is the normalized control current, I_{IFL} is the total current in the presence of ifenprodil, [IFL] is the concentration of ifenprodil, IC_{50_1} and IC_{50_2} are the concentrations that inhibited 50% of the current, and A_1 and A_2 are the coefficients of the two components. As shown by the fitted curve in Fig. 2B, the two components were responsible for approximately equal proportions of the antagonism (A_1 = 0.51 and A_2 = 0.49), with IC_{50} values of 0.75 and 161 μM.

The recovery after ifenprodil application had two distinct components at high concentrations, a rapid phase followed by a slow relaxation (see Fig. 2A). However, the proportion of the blocked current that recovered at a slow rate did not increase for [IFL] of >10 μM. The amount of current subject to slow recovery was estimated by measurement of the residual inhibition at 1 sec after washout of ifenprodil. The residual inhibition was 0.42 ± 0.03 (n = 9), 0.44 ± 0.06 (n = 12), and 0.43 ± 0.06 (n = 4) for 30, 100, and 300 μM ifenprodil, respectively (Fig. 2B). This is nearly the same as the inhibition due to the high affinity component of the concentration-response curve and suggests that the slow relaxation represents recovery from high affinity block.

Macroscopic kinetics of ifenprodil block also had two components. The rate of onset of inhibition increased with the ifenprodil concentration. The onset for five concentrations of ifenprodil (0.3–30 μM), during the continuous application of NMDA, is shown in Fig. 3A. At low concentrations, the onset was quite slow and was well fitted by a single-exponential function (τ_{on_1}), ranging from 7.5 ± 0.2 sec at 0.3 μM (n = 4) to 1.4 ± 0.3 sec at 10 μM (n = 8). The concentration dependence of τ_{on_1} is shown in Fig. 3B. For concentrations of ≥30 μM, two exponentials were required to fit the onset; at 30 μM, τ_{on_1} was 416.7 ± 57.6 msec and τ_{on_2} was 44.8 ± 12.1 msec (n = 9). However, as τ_{on_2} approached the drug delivery rate at high concentrations (≈20 msec at 100 μM ifenprodil), it is likely that we underestimated the time constant for the fast component. The two kinetic components of the onset suggest that separate processes may contribute to antagonism, one of which becomes apparent only at ifenprodil concentrations above 10 μM. This is consistent with the two components of inhibition seen in the concentration-response curve (see Fig. 2).

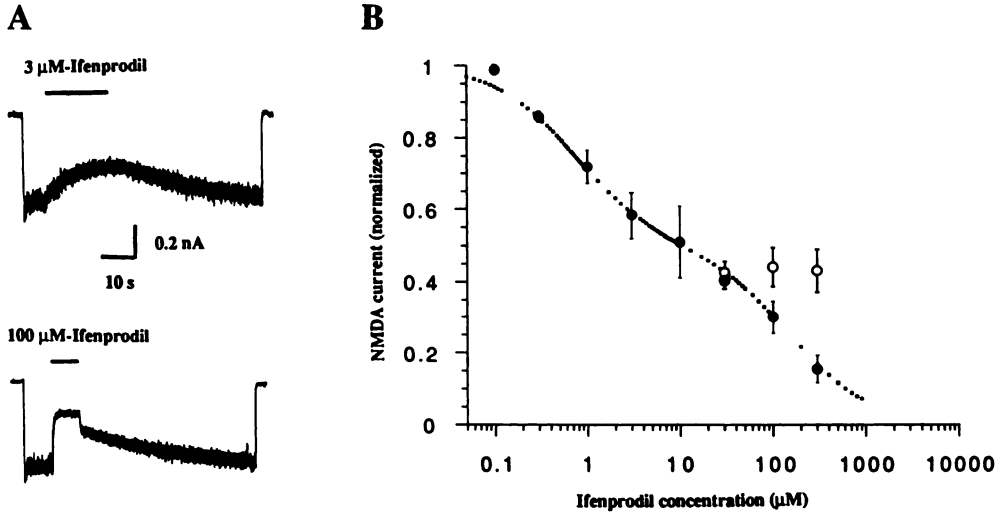

Fig. 2. A, Responses to NMDA (10 μM) in the presence of 3 and 100 μM ifenprodil are shown for one neuron at a holding potential of −50 mV. B, Maximum inhibition during ifenprodil application (●) was fitted with the sum of two single-binding site absorption isotherms. The IC_{50} values were 0.75 and 161 μM, with coefficients of 0.51 and 0.49, respectively. ○, Residual inhibition immediately after the fast component of recovery. Data points are the average ± standard deviation of 4 to 16 cells.

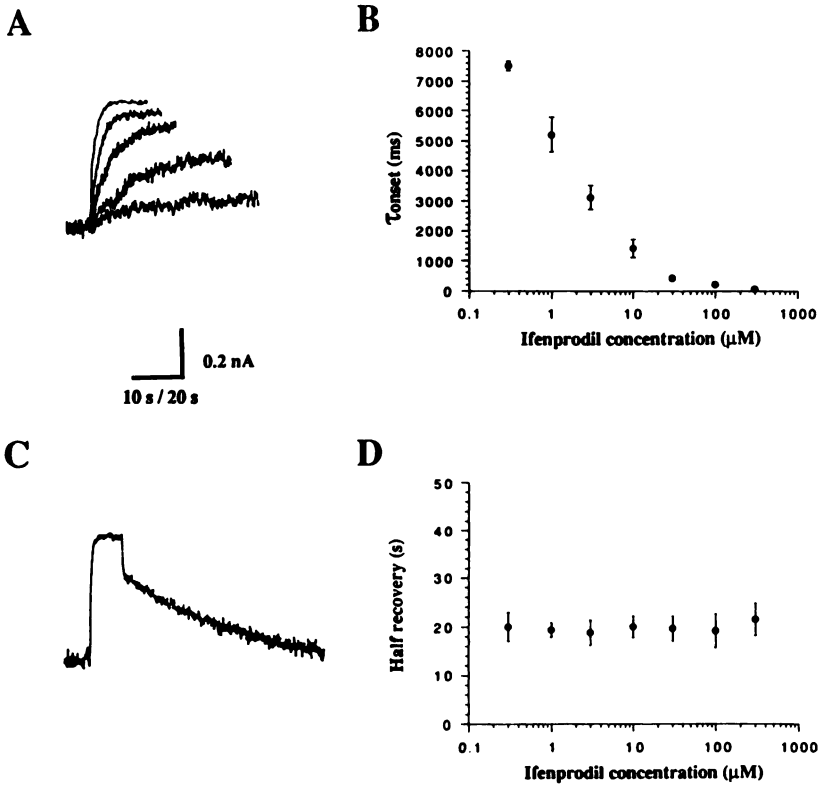

Fig. 3. A, The onset of inhibition for 0.3, 1, 3, 10, and 30 μM ifenprodil is shown for one neuron at a holding potential of −50 mV. B, At concentrations lower than 10 μM, the onset was well fitted by a single exponential, which became faster with increasing concentrations. A second exponential was required to fit the onset for high concentrations of ifenprodil, but only the slow time constant is plotted in B (see text). C, The rate of recovery from ifenprodil (100 μM) also had two components. The fast recovery was apparent only at >10 μM ifenprodil. D, The slow recovery rate was independent of ifenprodil concentration. The data were filtered at 1 kHz for curve fitting; slow onsets were filtered at 10 Hz for display. Data in B and D are the average of 4 to 12 cells.

The recovery from inhibition also showed two components. At low concentrations, only a slow recovery could be observed (see, e.g., Fig. 2A); for 3 μM ifenprodil, the half-recovery time was 18.8 ± 2.6 sec (n = 8). As shown in Fig. 3C, an additional fast recovery become apparent at higher concentrations of ifenprodil, with a time constant of ≈30 msec. In contrast to the rate of onset, neither component of the recovery was concentration dependent, as shown for the slow recovery rate in Fig. 3D. The fast recovery was well fitted with single-exponential functions. The fast recovery time constants at ifenprodil concentrations of 30, 100, and 300 μM were 31.1 ± 17.1 (n = 9), 30.1 ± 13.2 (n = 12), and 31.2 ± 8.3 (n = 4) msec, respectively.

The rapid onset and slow recovery with ifenprodil resemble the action of some open-channel blockers, such as MK-801 (24). Slow open-channel-blocking drugs show use dependence, and recovery from block is increased by re-exposure to the agonist. However, inhibition of NMDA current did not increase during prolonged applications of ifenprodil (Fig. 4A). In addition, pre-exposure to ifenprodil shortly before application of NMDA also antagonized the inward current, suggesting that ifenprodil can act on NMDA receptors that are not open. As shown in Fig. 4B, a 10-sec exposure to ifenprodil resulted in a 50% block of the response, even at a positive holding potential (+40 mV). Repeated applications of agonist revealed a half-recovery time of ≈20 sec and full recovery at 90 sec (Fig. 4B). However, recovery did not depend on channel activity, inasmuch as a similar recovery was seen when NMDA was applied 90 sec after initial exposure to ifenprodil (Fig. 4C). Similar results were obtained on five neurons.

Calcium-dependent inactivation and high affinity ifenprodil block are not additive. Inactivation or desensitization of NMDA currents has several components, one of which is calcium dependent (21, 25, 26). Calcium-dependent inactivation is voltage dependent and virtually absent when

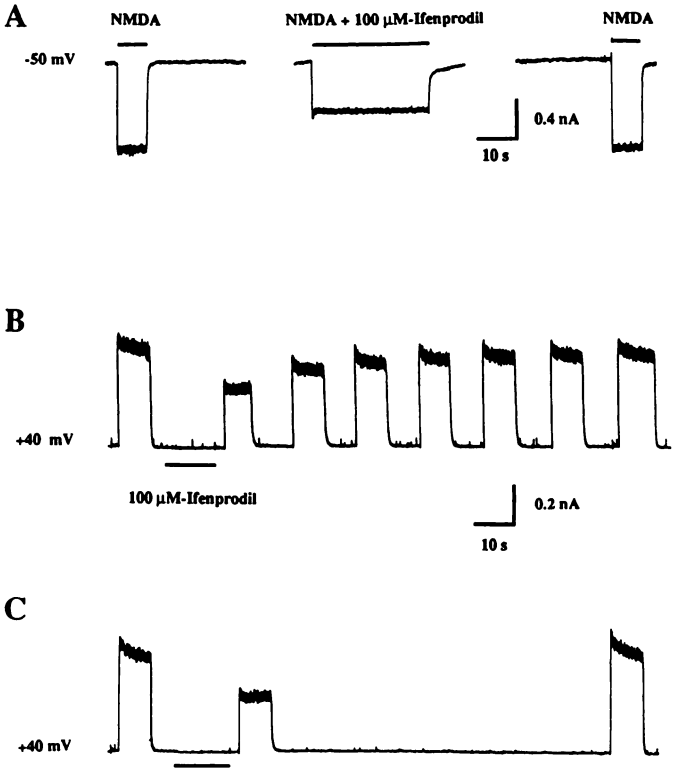

Fig. 4. A, Inward current evoked by NMDA (10 μM) before and during a 30-sec application of ifenprodil (100 μM). Inhibition did not increase during the long application and showed full recovery. B, A 15-sec application of ifenprodil in the absence of NMDA resulted in inhibition of the subsequent responses, followed by a slow recovery. C, The same protocol as in B was used, except only one application of NMDA was given during the recovery period, demonstrating that the recovery rate is not dependent on reopening of the channels. The holding potential was +40 mV in B and C. The extracellular solution contained 1.3 mM $[Ca^{2+}]_o$.

$[Ca^{2+}]_o$ is <0.3 μM (22). It became apparent that the degree of inhibition by ifenprodil was highly dependent on the external calcium concentration. In 1.3 mM $[Ca^{2+}]_o$, the NMDA-induced current was followed by a slowly developing relaxation, which reached a steady state level within 10–20 sec, consistent with calcium-dependent inactivation (Fig. 5A). Under these conditions, ifenprodil blocked 43 ± 4% of the steady state current (n = 8). However, in 0.3 mM $[Ca^{2+}]_o$, calcium-dependent inactivation was minimal, and 70 ± 4.6% of the steady state current was blocked by ifenprodil (n = 16). Therefore, the ifenprodil-resistant current was approximately 20–30% of the initial peak current regardless of $[Ca^{2+}]_o$, as shown for the same neuron in Fig. 5A. Likewise, when calcium-dependent inactivation was prevented by holding the membrane potential at +40 mV, antagonism by ifenprodil in 1.3 mM $[Ca^{2+}]_o$ was similar to that observed in low external Ca^{2+} (Fig. 5B). This suggests that channels inactivated by Ca^{2+} cannot be further inhibited by ifenprodil and that the apparent voltage dependence of ifenprodil action in 1.3 mM $[Ca^{2+}]_o$ simply reflects the presence of calcium-dependent inactivation.

The concentration-response curve was modified when $[Ca^{2+}]_o$ was increased from 0.3 to 1.3 mM (Fig. 6). The solid line shows the best fit to the data of Fig. 2 in 0.3 mM $[Ca^{2+}]_o$. In the presence of 1.3 mM $[Ca^{2+}]_o$, the concentration-response

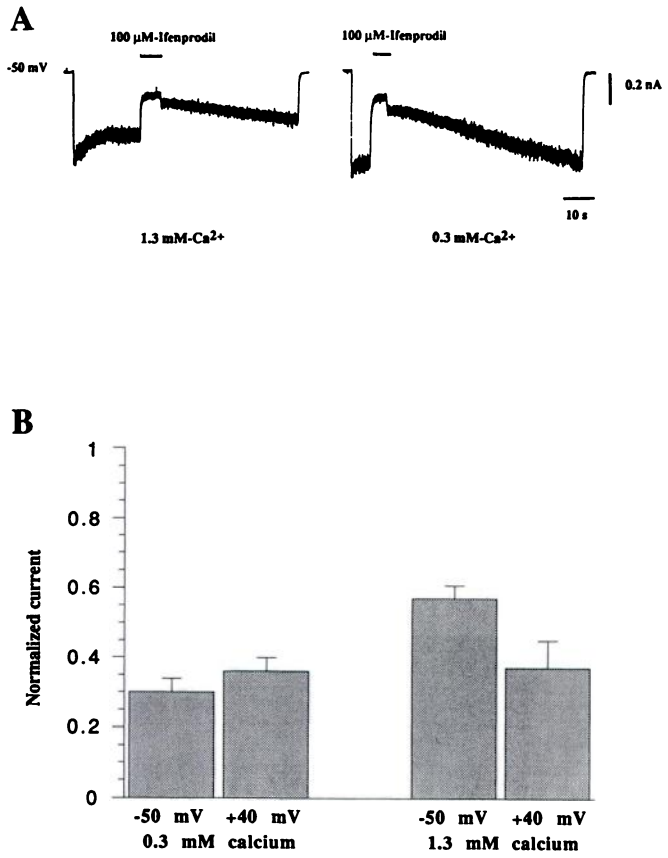

Fig. 5. A, Ifenprodil (100 μM) was applied in the presence of 1.3 mM $[Ca^{2+}]_o$ (*left*) or 0.3 mM $[Ca^{2+}]_o$ (*right*) after the NMDA-evoked current reached a steady state. Note the calcium-dependent inactivation of the NMDA-evoked current in 1.3 mM $[Ca^{2+}]_o$. The ifenprodil-resistant current was similar in 0.3 mM and 1.3 mM $[Ca^{2+}]_o$. The holding potential was −50 mV. B, The histograms show the inhibition of NMDA responses at holding potentials of −50 and +40 mV. Ifenprodil inhibition showed an apparent voltage dependence in 1.3 mM $[Ca^{2+}]_o$. NMDA responses were normalized to the steady state immediately preceding ifenprodil application.

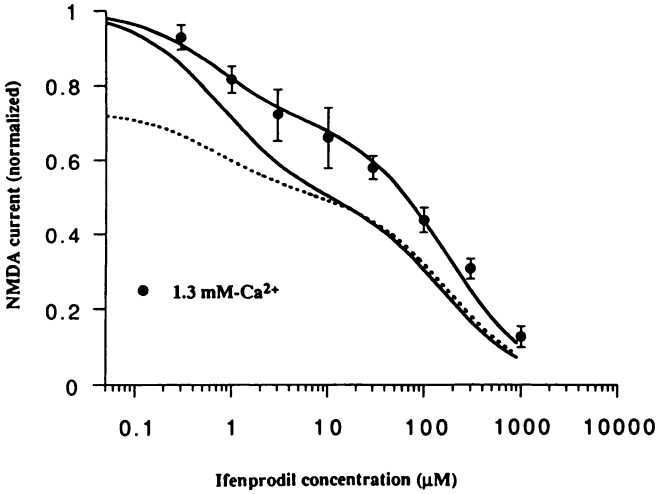

Fig. 6. The ifenprodil concentration-response curve in the presence of 1.3 mM $[Ca^{2+}]_o$ (●) was fitted with the sum of two single-binding site isotherms, as in Fig. 2. Each point was normalized to the steady state NMDA current preceding ifenprodil application. The IC_{50} values were 0.75 and 200 μM, similar to those seen in low calcium (0.3 mM; see Fig. 2). However, the proportion of inhibition due to the high affinity component was reduced from 0.51 to 0.31. The concentration-response curve for low calcium (——) is replotted from Fig. 2 for comparison. (· · · ·), Best fit to the data in 1.3 mM $[Ca^{2+}]_o$, normalized to the initial peak inward current, demonstrating that only the high affinity component is reduced after calcium-dependent inactivation of the NMDA current.

curve, normalized to the steady state current preceding ifenprodil application, could still be fitted with the sum of two binding site isotherms. IC_{50_1} was 0.75 μM and IC_{50_2} was 200 μM. Although the IC_{50} values were similar, the contribution of the two components of inhibition was altered by increases in extracellular calcium. Whereas in 0.3 mM $[Ca^{2+}]_o$ the high and low affinity components were each responsible for approximately 50% of the total inhibition (see Fig. 2B), in 1.3 mM $[Ca^{2+}]_o$ the coefficients of the binding site isotherm were 0.31 for the high affinity component and 0.69 for the low affinity component. Inasmuch as the calcium-dependent inactivation reduced the NMDA current in 1.3 mM $[Ca^{2+}]_o$ to approximately 75% of control (e.g., Fig. 5A), the change in the coefficients in 1.3 mM $[Ca^{2+}]_o$ most likely reflects a decrease in the high affinity component. This was readily apparent when the ifenprodil inhibition curve in 1.3 mM $[Ca^{2+}]_o$ was normalized to the steady state current immediately preceding ifenprodil application (Fig. 6), suggesting that the high affinity action of ifenprodil is not additive with calcium-dependent inactivation.

Ifenprodil reduced the activity of single NMDA channels. The effects of ifenprodil on single NMDA-activated channels were examined in outside-out patches pulled from cultured hippocampal neurons. In the presence of NMDA, well resolved, large conductance openings were observed, as shown for one patch in Fig. 7A, at a holding potential of −50 mV. In the same patch, ifenprodil (3 μM) produced a dramatic reduction in the number of channel openings, with no apparent effect on the single-channel conductance (Fig. 7B). Recovery of channel activity required 2–3 min after drug exposure, consistent with the slow recovery seen in whole-cell experiments (e.g., compare Figs. 1A and 9A).

Amplitude histograms for one patch in the presence and absence of ifenprodil are shown in Fig. 8, A and B. NMDA-activated channels had several conductance levels, as previously described (27, 28). For six patches, the levels were 50.0 ± 1.7, 38.7 ± 1.8, 28.9 ± 1.7, and 15.1 ± 1.8 pS. Although ifenprodil

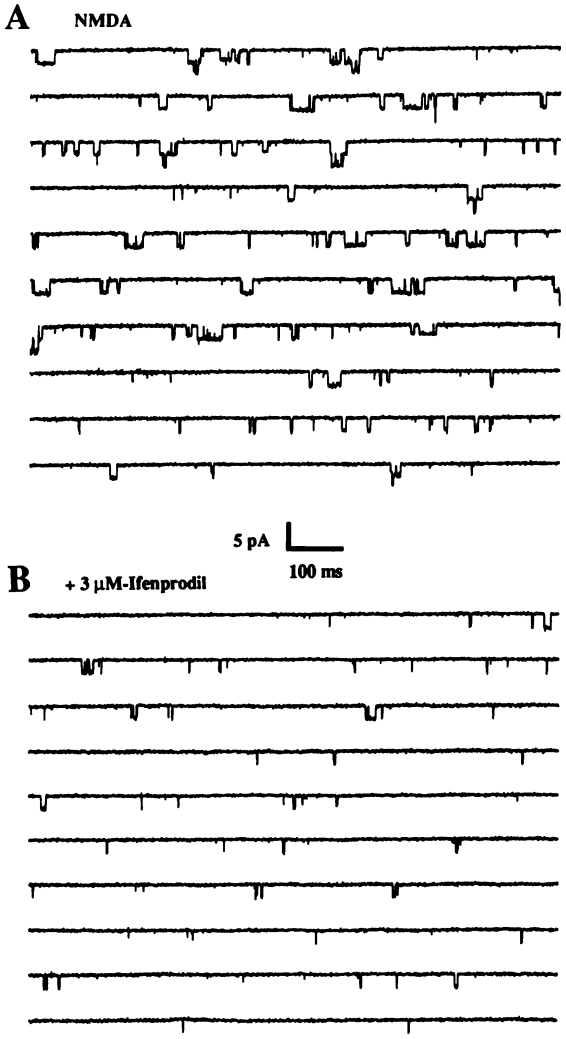

Fig. 7. Single-channel currents were evoked by application of 2 μM NMDA to an outside-out patch at a holding potential of −50 mV. Epochs of 10 sec, containing clearly resolved NMDA channel openings, are shown for one patch in the absence (A) and presence (B) of ifenprodil (3 μM). Note the decrease in number of events and the duration of the openings in the presence of ifenprodil. The extracellular solution contained 500 nM glycine and 1.3 mM Ca^{2+}. The data were filtered at 2 kHz.

(3 μM) reduced the number of openings, there was no effect on the single-channel conductances; mean conductance levels were 49.0 ± 1.0, 39.1 ± 1.7, 27.6 ± 2.0, and 17.0 ± 1.0 pS. However, ifenprodil did affect the open time of NMDA channels. The open time histograms for the large conductance levels (>35 pS) are shown for one patch in Fig. 8, C and D. In the absence of ifenprodil, the open time histograms were fitted with the sum of two exponentials with time constants of 1.7 ± 0.7 and 7.5 ± 1.2 msec (n = 33). In 3 μM ifenprodil, the long open time was reduced. For eight patches, τ_1 was 1.7 ± 0.5 and τ_2 was 3.5 ± 0.9 msec. The reduction in the long mean open time was voltage independent; at a holding potential of +40 mV, τ_1 was 1.5 ± 0.3 msec and τ_2 was 3.6 ± 0.7 msec (n = 4).

The analysis of mean open time included all events lasting more than 200 μsec. The reduction in τ_2 by ifenprodil can be more clearly defined using burst analysis. Closed time histograms at −50 mV were fit by the sum of three or four exponentials; the short closed time (0.56 ± 0.1 msec, n = 33) was constant between patches and was unaffected by 3 μM ifenprodil (0.63 ± 0.1 msec, n = 8). Thus, the critical gap duration was defined as 3 times the short closed interval; events shorter than the critical gap were excluded from the burst analysis (29). For six patches, burst duration histograms were fitted with the sum of three exponentials (0.3 ± 0.1, 3.0 ± 0.9, and 21.0 ± 3.4 msec). In the presence of ifenprodil, only the long burst duration was significantly reduced (0.3 ± 0.2, 2.4 ± 0.8, and 7.8 ± 1.3 msec). The reduction in the mean open time and long duration bursts suggests a kinetic scheme in which ifenprodil permits exit from the open state to an inactivated or closed state. The rate constant was estimated from the slope of the relationship between the inverse of the mean open time and the ifenprodil concentration (Fig. 9B). At a holding potential of −50 mV, the slope was 6.045×10^7 $M^{-1}sec^{-1}$.

To compare the antagonism of single-channel activity with inhibition of the whole-cell current, amplitude histograms were constructed using a point-by-point method. The open probability, obtained from the normalized area of the histogram, was reduced with increasing ifenprodil concentrations (Fig. 9C). Surprisingly, low concentrations of ifenprodil blocked a much larger proportion of the current than in whole-cell recording in normal 1.3 mM $[Ca^{2+}]_o$. Ifenprodil (3 μM) produced a 62 ± 11% (n = 6) reduction of the open probability but only a 27% reduction in the whole-cell current (see Fig. 6).

At high concentrations, ifenprodil acts as a glycine antagonist. Both the concentration-response curve and the macroscopic kinetics are consistent with a two-component action of ifenprodil. We examined whether the low affinity component could be due to an interaction with the strychnine-insensitive glycine modulatory site on the NMDA receptor (30). Glycine binding is an absolute requirement for channel activation, and a number of compounds act as glycine antagonists (31–33). As expected, increasing the extracellular glycine concentration increased the initial peak current response to NMDA at a holding potential of −50 mV. However, increases in glycine reduced the inhibition produced by 100 μM ifenprodil (Fig. 10A). In the presence of 150 nM glycine ifenprodil reduced the NMDA current to 20.8 ± 5.4% of control (V_h = −50 mV, n = 8), but in the presence of 10 μM glycine the NMDA current was reduced to only 72.9 ± 4.4% of control (V_h = −50 mV, n = 7). Similar effects were seen at a holding potential of +40 mV (Fig. 10).

The concentration-response curve for glycine potentiation of the NMDA current is shown in Fig. 11. A 50 nM residual concentration of glycine was incorporated into the final concentration, based on the responses observed in nominally glycine-free solutions. The data could be fitted with the logistic equation, in the absence of ifenprodil, with an EC_{50} of 195 nM and a Hill coefficient of 1.3. Ifenprodil caused a rightward shift of the glycine concentration-response curve, but high concentrations of glycine could not completely overcome ifenprodil inhibition (Fig. 11A). The residual inhibition was approximately 30% in the presence of either 3 or 100 μM ifenprodil, which is the same proportion of antagonism due to the high affinity ifenprodil component in 1.3 mM $[Ca^{2+}]_o$. Thus, the action of low concentrations of ifenprodil was glycine independent. To examine the interaction of ifenprodil with glycine binding, the residual glycine-independent inhibition was removed by normalizing the data to the maximum NMDA-evoked current at 100 μM glycine. The glycine-dependent inhibition was well described by a competitive inhibition model with an IC_{50} of 55 μM for ifenprodil (Fig. 11B), suggesting that the low

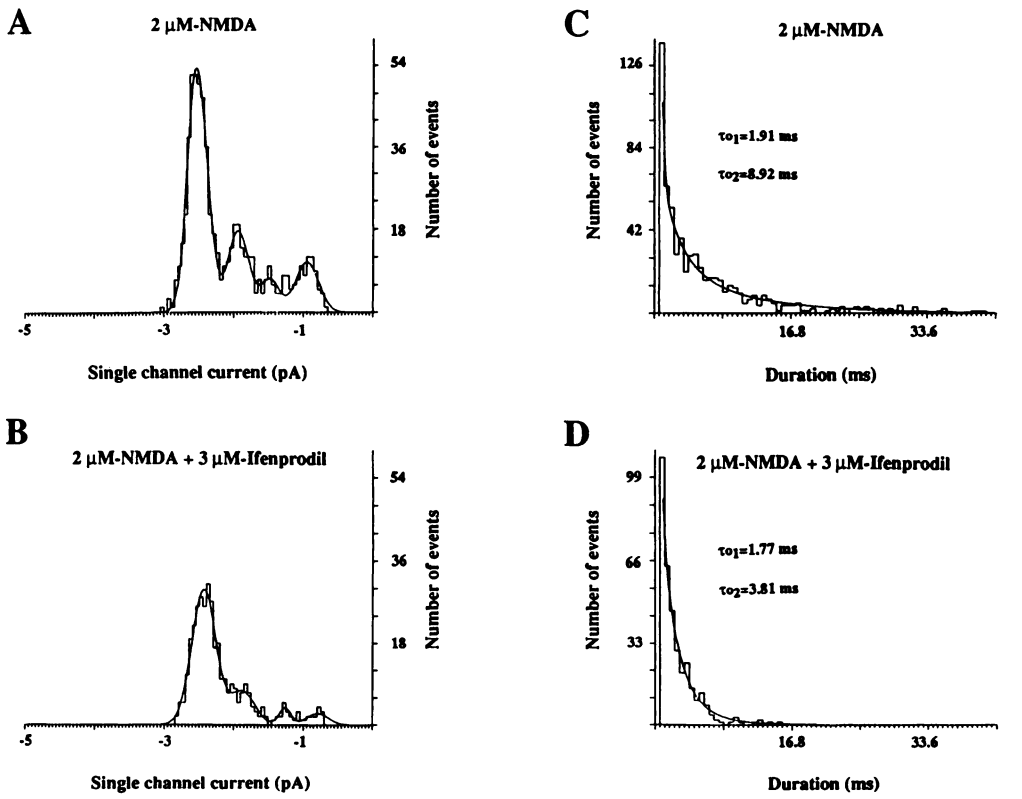

Fig. 8. A, Amplitude histograms for one patch were fitted with the sum of four gaussian functions, with average peak currents of 2.5, 1.9, 1.5, and 0.9 pA. The extracellular solution contained 2 μM NMDA, 500 nM glycine, and 1.3 mM Ca^{2+}. B, In the presence of ifenprodil (3 μM), single-channel current amplitudes were unchanged. For this patch, the mean amplitudes were 2.4, 1.9, 1.3, and 0.9 pA. Open time histograms of the large conductance openings (>35 pS) for the same patch are shown in the absence (C) and presence (D) of ifenprodil. The long mean open time was decreased. Open time histograms were fitted with the sum of two exponentials, using a bin-width of 0.6 msec.

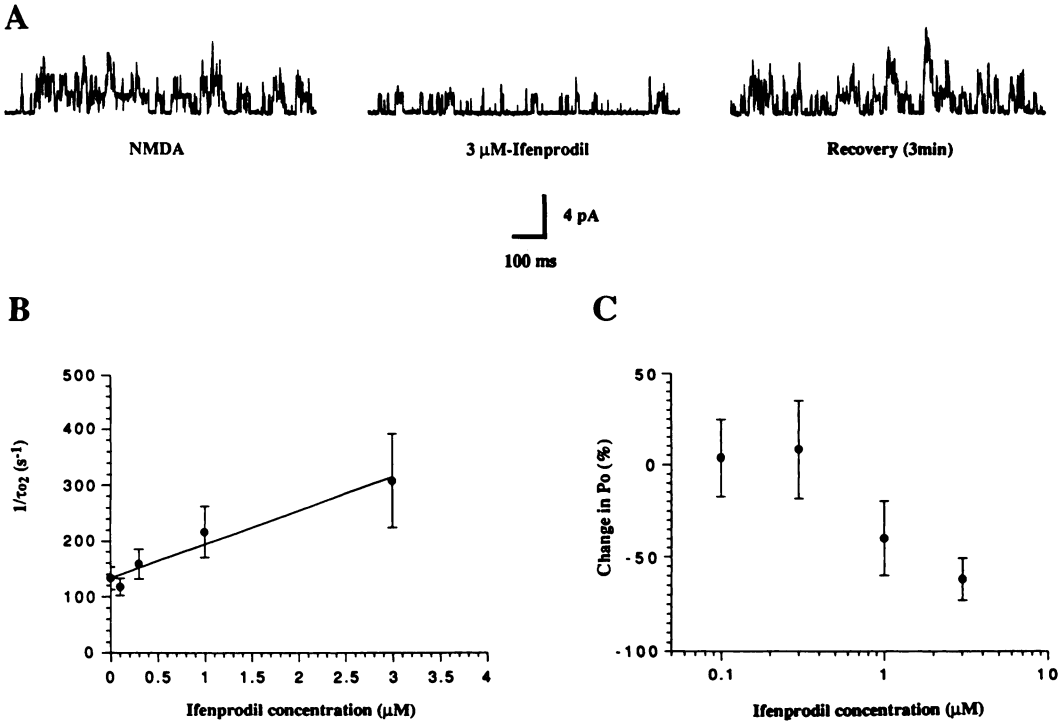

Fig. 9. A. Outward currents through NMDA channels in an outside-out patch at a holding potential of −50 mV are shown. Ifenprodil (3 μM) reduced channel activity, which fully recovered after 3 min. B, The inverse of the long mean open time was plotted as a function of the concentration of ifenprodil. The data could be fitted with a regression line with a slope of 6.045×10^7 $M^{-1}sec^{-1}$. The value of $1/\tau_{o_2}$ for [ifenprodil] = 0 was 133.1 ± 20.3 sec^{-1} (n = 33), corresponding to a mean open time of 7.51 msec. C, The open probability (P_o) for NMDA channels (as defined in Materials and Methods) was plotted as a function of ifenprodil concentration. Ifenprodil (3 μM) resulted in a 62 ± 11% decrease in P_o (n = 6). Data points are the average of five to eight patches.

affinity component of ifenprodil inhibition results from antagonism at the glycine binding site on the NMDA receptor.

Discussion

Our results demonstrate that two components underlie ifenprodil inhibition of responses evoked by NMDA. At low concentrations ifenprodil appears to promote transitions to a nonconducting state of the channel, whereas at high concentrations ifenprodil acts as an allosteric inhibitor of glycine binding. The action of low concentrations of ifenprodil is distinct from that of previously described NMDA receptor antagonists.

Different mechanisms for the two components of inhibition. Prior binding and electrophysiological studies have suggested several possible mechanisms for the noncompetitive antagonist action of ifenprodil, including actions at the Zn^{2+}, polyamine, and glycine sites on the NMDA receptor (17, 34). The biphasic nature of the ifenprodil concentration-response

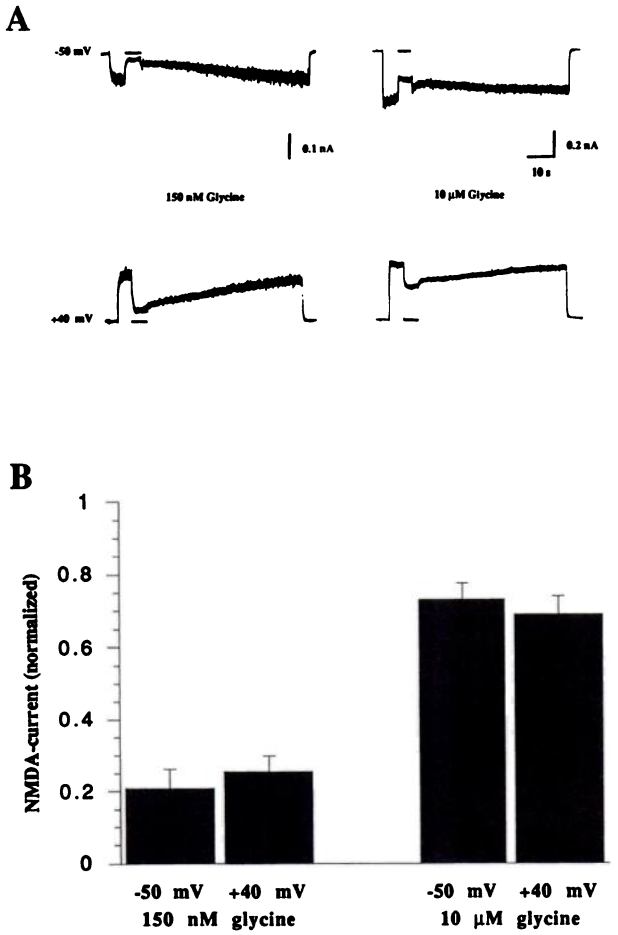

Fig. 10. A, Whole-cell responses to NMDA (10 μM) in 150 nM and 10 μM glycine are shown for one neuron at holding potentials of −50 mV and +40 mV. Ifenprodil block was larger in the low glycine solution at both holding potentials. B, Results for all neurons tested are summarized. The extracellular solution contained 1.3 mM Ca^{2+}.

curve in our experiments suggested the possibility of two separate mechanisms. In addition, the low and high affinity components also showed distinct macroscopic kinetics. The fast rates of onset and recovery could be attributed to the low affinity site, because they were present only at high concentrations of ifenprodil. Because the K_i values of the two components differed by 200-fold and the high affinity component did not completely block the NMDA-evoked current, it was possible to reliably separate the proportion of current blocked by the two components. Thus, the characteristics of the two components could be examined in relative isolation.

Glycine is a co-agonist at NMDA receptors (31); thus, glycine antagonism can be misinterpreted as noncompetitive NMDA antagonism (e.g., see Ref. 35). The glycine dependence of ifenprodil block could be clearly attributed to the low affinity site. First, low concentrations of ifenprodil could not be overcome even by supramaximal concentrations of glycine. Second, the proportion of current that was glycine independent was equal to the maximal inhibition due to the high affinity component. As a result, the rightward shift of the glycine dose-response curve by ifenprodil appears to be consistent with a weak competitive action on the glycine binding site. However, if this were truly a competitive interaction, the on-rate of ifenprodil would be limited by the dissociation rate of bound glycine molecules, which is approximately 300 msec (36). Although we were unable to determine the true rate constants for the low affinity site, both the fast on- and off-rates were much faster than 300 msec and approached the rate of solution exchange (20–30 msec). The most likely possibility is that ifenprodil binding results in an allosteric decrease in the affinity of glycine binding, e.g., the approximate 5-fold rightward shift in the glycine dose-response curve would then predict a dissociation rate of glycine of ≈60 msec, assuming the association rate was unaffected. This is near the observed value of 20 msec for the fast onset time constant for ifenprodil. The low affinity of this interaction may explain why this has not been detected in binding studies (34) (but see Ref. 37). However, it is unlikely that the low affinity action seen in our experiments will contribute significantly to ifenprodil block of NMDA channels *in vivo*, due to the high ambient concentrations of glycine (30, 38).

The high affinity binding site. The effects of low concentrations of ifenprodil had several unique features, compared with those of other NMDA receptor antagonists. The recovery rate of the macroscopic current was extremely slow, with a time constant of approximately 30 sec. Similar slow recovery rates have been observed with highly potent channel-blocking drugs, such as ketamine or MK-801 (24, 39, 40), but the recovery for ifenprodil was voltage independent. The onset time constant was also slow but was dependent on ifenprodil concentration, consistent with a bimolecular reaction between ifenprodil and the receptor. Assuming that drug binding is slow with respect to channel opening (see Ref. 24), the K_i can be estimated from the onset (τ_{onset}) and recovery ($\tau_{recovery}$) of the macroscopic current, where

$$K_i = (\tau_{onset} \cdot [IFN])/\tau_{recovery}$$

For 1 μM ifenprodil, the onset time constant was 5.3 sec, giving a calculated K_i of 180 nM. This is in reasonable agreement with our measured IC_{50} of 750 nM. Several experiments exclude the possibility that ifenprodil acts as a conventional open channel blocker. Low concentrations of ifenprodil were not voltage or use dependent, as occurs with ketamine (39, 40); thus, the site of action is unlikely to be within the membrane electric field. Likewise, NMDA-evoked responses on neurons preexposed to ifenprodil were also inhibited, providing clear evidence that ifenprodil binding does not require either agonist binding or channel opening.

An estimate of the kinetics of this interaction could be derived from single-channel experiments. Like Zn^{2+}, a voltage-independent NMDA antagonist, low concentrations of ifenprodil reduced the frequency of channel opening and the mean open time, without altering the single-channel conductance. Recovery of channel activity was slow, with a rate similar to the slow recovery rate of the macroscopic current. The decrease in mean open time with increasing ifenprodil concentration was used to estimate the apparent blocking rate constant, as has been done for other noncompetitive NMDA antagonists, including Mg^{2+}, MK-801, and Zn^{2+} (18, 24, 41). The inactivation rate constant was relatively fast, $\approx 6 \times 10^7$ M^{-1} sec^{-1}, suggesting that ifenprodil binding is limited primarily by diffusion. This rate is similar to those of Mg^{2+} (1.6×10^7 M^{-1} sec^{-1}) (40) and MK-801 (3×10^7 M^{-1} sec^{-1}) (23) but 10 times faster than that of Zn^{2+} (4×10^6 M^{-1} sec^{-1}). An additional difference between ifenprodil and Zn^{2+} was apparent from analysis of the open time histograms. Whereas Zn^{2+} reduced both the short and long open times (18), ifenprodil had no effect on the short open time. This may suggest the existence of two distinct open states,

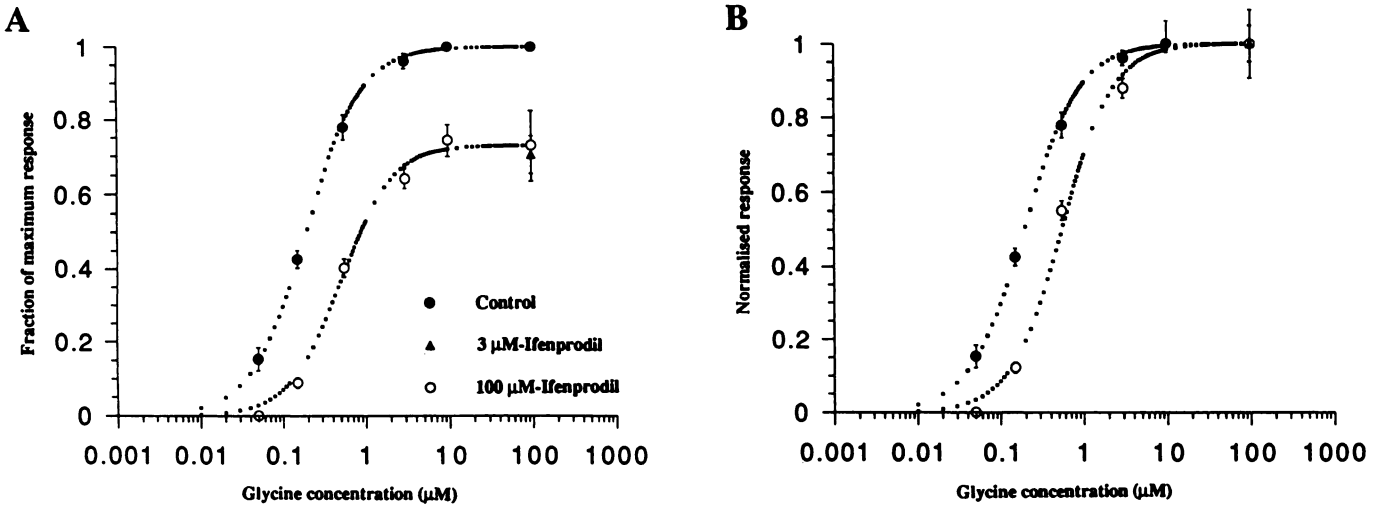

Fig. 11. A, Glycine concentration-response curves were plotted in the absence (●) and presence of 3 μM (▲) and 100 μM (○) ifenprodil. The control data were fitted using least-squares methods to the equation $I = I_{max}/(1 + (EC_{50}/[Gly]^n)$, where I is the NMDA current, I_{max} is the maximum response, [Gly] is the glycine concentration, EC_{50} is the glycine concentration that produces a half-maximal response, and n is the Hill coefficient. The EC_{50} was 195 nM and the Hill coefficient was 1.3. In the presence of 100 μM ifenprodil, the curve was shifted to the right, but supramaximal concentrations of glycine could not completely overcome the inhibition. The data were fitted with a competitive model, assuming a glycine-independent component of inhibition (see text). The curve is the least squares fit to the equation $I = I_{max}/(1 + (EC_{50}(1 + ([IFL]/IC_{50}))/[Gly]^n)$, where [IFL] is the ifenprodil concentration and IC_{50} is the concentration of ifenprodil that produced a half-maximal block. The IC_{50} was 55 μM. B, The data shown in A were normalized and replotted to show the glycine-sensitive component in the absence (●) and presence (○) of ifenprodil (100 μM). The estimated residual glycine concentration in nominally glycine-free solutions was 50 nM. Data shown are mean of 4 to 12 cells.

only one of which is affected by ifenprodil. It is tempting to speculate that this may explain why low concentrations of ifenprodil do not produce complete inhibition.

Is ifenprodil a polyamine antagonist? A polyamine-sensitive site on the NMDA receptor has been proposed, based on the potentiation of [^{3}H]MK-801 binding by spermine and spermidine (14). Several other di- and triamines have shown partial agonist or antagonistic action in this assay (17, 42, 43). NMDA responses on cultured hippocampal neurons and mRNA-injected *Xenopus* oocytes have also been potentiated by extracellular application of spermine and spermidine (15, 16, 43). Ifenprodil has been reported to antagonize the spermine-induced increases in [^{3}H]TCP and, thus, to be a polyamine antagonist (12) (but see Ref. 16). We attempted to test this possibility using the competitive polyamine antagonist DET (43). On five neurons, DET (150 μM) had no effect on the ifenprodil inhibition of NMDA-evoked currents. DET also had no direct action on NMDA currents. Thus, the effects of ifenprodil in our experiments cannot be explained by antagonism of endogenous polyamines at an extracellular site on the receptor.

Recently, both binding and physiological evidence have suggested that polyamines increase the affinity of glycine binding to the NMDA receptor (44). In our experiments, low concentrations of ifenprodil had no effect on the EC_{50} of the glycine concentration-response curve, although the low affinity action of ifenprodil did cause a rightward shift of the curve. We suspect that any apparent interaction between polyamines and ifenprodil occurs via the glycine modulatory site. However, it is curious that polyamines, which are predominantly intracellular constituents (45), would bind under physiological conditions at an extracellular site. In addition, polyamines are polyvalent cations and, thus, may have different actions in the low ionic strength buffers used in binding assays, compared with physiological saline. Of note, Reynolds (46) failed to demonstrate polyamine potentiation of NMDA responses using fura-2 measurements in cultured forebrain neurons.

Calcium-dependent inactivation. An interesting characteristic of high affinity ifenprodil block is the nonadditivity with calcium-dependent inactivation. Inactivation of NMDA channels by calcium has been shown to be voltage dependent and appears to result from increases in cytoplasmic calcium (21, 25, 47). This inactivation has a relatively slow onset ($\tau \approx$ 3–5 sec) and can be differentiated from glycine-dependent desensitization (22) and from the rundown or washout of NMDA responses in whole-cell or outside-out recording (26, 48). The mechanism by which Ca^{2+} acts to inactivate the channel is unclear. Although calcium-dependent inactivation and low concentrations of ifenprodil result in incomplete block of the NMDA-evoked current and involve slow macroscopic kinetics, the mechanisms of action would appear to be different. Calcium did not shift the IC_{50} for the high affinity ifenprodil site, suggesting that calcium does not directly compete with ifenprodil binding. Several other observations suggest that ifenprodil does not share identical mechanisms with calcium. First, calcium must act intracellularly, whereas ifenprodil appears to bind to an extracellular site. Second, ifenprodil inhibition is not completely occluded by previous calcium-dependent inactivation.

Low concentrations of ifenprodil produced a greater maximal inhibition of NMDA channels in steady state recording from outside-out patches, compared with the macroscopic current. Because these experiments were performed in normal extracellular Ca^{2+}, it might have been expected that ifenprodil would produce only a small inhibition. It is possible either that more effective dialysis in the patch removed the necessary constituents for calcium-dependent inactivation or that calcium buffering was more efficient. In any case, it suggests that the functional state of the NMDA channel may dramatically alter the action of antagonists such as ifenprodil. Although further experiments are necessary to define the inactivation mechanisms of the NMDA channel, it seems likely that ifenprodil and calcium, acting at different sites, may reveal alternative

modes of gating. Such alterations in gating may also underlie the incomplete inhibition of voltage-dependent calcium channels by neurotransmitters (49).

Acknowledgments

We thank J. Volk for preparing the cell cultures, Dr. B. Scatton (Synthelabo) for the gift of ifenprodil, and Drs. M. Mayer and C. Jahr for reading an earlier version of the manuscript.

References

1. Rothman, S. M., and J. W. Olney. Glutamate and the pathophysiology of hypoxic-ischemic brain damage. *Ann. Neurol.* **19**:105–111 (1986).
2. Choi, D. W. Glutamate neurotoxicity and diseases of the nervous system. *Neuron* **1**:623–634 (1988).
3. Rothman, S. M., and D. W. Choi. The role of glutamate neurotoxicity in hypoxic-ischemic neuronal death. *Annu. Rev. Neurosci.* **13**:171–182 (1990).
4. MacDermott, A. B., M. L. Mayer, G. L. Westbrook, S. J. Smith, and J. L. Barker. NMDA-receptor activation increases cytoplasmic calcium concentration in cultured spinal cord neurones. *Nature (Lond.)* **321**:519–522 (1986).
5. Choi, D. W. Ionic dependence of glutamate neurotoxicity. *J. Neurosci.* **7**:369–379 (1987).
6. Collingridge, G. L., and R. A. J. Lester. Excitatory amino acid receptors in the vertebrate central nervous system. *Pharmacol. Rev.* **40**:143–210 (1989).
7. Willetts, J., R. L. Balster, and J. D. Leander. The behavioral pharmacology of NMDA receptor antagonists. *Trends Pharmacol.* **11**:423–428 (1990).
8. Carron, C., A. Jullien, and B. Bucher. Synthesis and pharmacological properties of a series of 2-piperidino alkanol derivatives. *Arzneim.-Forsch. Drug Res.* **21**:1992–1998 (1971).
9. Cook, P., and I. James. Cerebral vasodilators. *N. Engl. J. Med.* **305**:1560–1564 (1981).
10. Gotti, B., D. Duverger, J. Bertin, C. Carter, R. Dupont, J. Frost, B. Gaudilliere, E. T. MacKenzie, J. Rousseau, B. Scatton, and A. Wick. Ifenprodil and SL 82.0715 as cerebral anti-ischemic agents. I. Evidence for efficacy in models of focal cerebral ischemia. *J. Pharmacol. Exp. Ther.* **247**:1211–1221 (1988).
11. Carter, C., J. Benavides, P. Legendre, J. D. Vincent, F. Noel, F. Thuret, K. G. Lloyd, S. Arbilla, B. Zivkovic, E. T. MacKenzie, B. Scatton, and S. Z. Langer. Ifenprodil and SL 82.0715 as cerebral anti-ischemic agents. II. Evidence for *N*-methyl-D-aspartate receptor antagonist properties. *J. Pharmacol. Exp. Ther.* **247**:1222–1232 (1988).
12. Carter, C., J. P. Rivy, and B. Scatton. Ifenprodil and SL 82.0715 are antagonists at the polyamine site of the *N*-methyl-D-aspartate (NMDA) receptor. *Eur. J. Pharmacol.* **164**:611–612 (1989).
13. Schoemaker, H., J. Allen, and S. Z. Langer. Binding of [^{3}H]ifenprodil, a novel NMDA antagonist, to a polyamine-sensitive site in the rat cerebral cortex. *Eur. J. Pharmacol.* **176**:249–250 (1990).
14. Ransom, R. W., and N. L. Stec. Cooperative modulation of [^{3}H]MK-801 binding to the *N*-methyl-D-aspartate receptor-ion channel complex by L-glutamate, glycine and polyamines. *J. Neurochem.* **51**:830–836 (1988).
15. Sprosen, T. S., and G. N. Woodruff. Polyamines potentiate NMDA induced whole-cell currents in cultured striatal neurons. *Eur. J. Pharmacol.* **179**:477–478 (1990).
16. McGurk, J. F., R. S. Zukin, and M. V. L. Bennett. Polyamines potentiate NMDA responses of receptors expressed in *Xenopus* oocytes. *Proc. Natl. Acad. Sci. USA* **87**:9971–9974 (1990).
17. Reynolds, I. J., and R. J. Miller. Ifenprodil is a novel type of *N*-methyl-D-aspartate receptor antagonist: interaction with polyamines. *Mol. Pharmacol.* **36**:758–765 (1989).
18. Legendre, P., and G. L. Westbrook. The inhibition of single NMDA-activated channels by zinc ions on cultured rat neurones. *J. Physiol. (Lond.)* **429**:429–449 (1990).
19. Hamill, O. P., A. Marty, E. Neher, B. Sakmann, and F. J. Sigworth. Improved patch-clamp techniques for high-resolution current recording from cells and cell-free membrane patches. *Pflugers Arch.* **391**:85–100 (1981).
20. Vyklicky, L., Jr., M. Benveniste, and M. L. Mayer. Modulation of *N*-methyl-D-aspartic acid receptor desensitization by glycine in mouse cultured hippocampal neurones. *J. Physiol. (Lond.)* **428**:313–331 (1990).
21. Mayer, M. L., and G. L. Westbrook. The action of *N*-methyl-D-aspartic acid on mouse spinal neurons in culture. *J. Physiol. (Lond.)* **361**:65–90 (1985).
22. Mayer, M. L., L. Vyklicky, Jr., and J. Clements. Regulation of NMDA receptor desensitization in mouse hippocampal neurons by glycine. *Nature (Lond.)* **338**:425–427 (1989).
23. Patneau, D. K., and M. L. Mayer. Structure-activity relationships for amino acid transmitter candidates acting at *N*-methyl-D-aspartate and quisqualate receptors. *J. Neurosci.* **10**:2385–2399 (1990).
24. Huettner, J. E., and B. P. Bean. Block of *N*-methyl-D-aspartate-activated current by the anticonvulsant MK-801: selective binding to open channels. *Proc. Natl. Acad. Sci. USA* **85**:1307–1311 (1988).
25. Mayer, M. L., A. B. MacDermott, G. L. Westbrook, S. J. Smith, and J. L. Barker. Agonist- and voltage-gated calcium entry in cultured mouse spinal cord neurons under voltage clamp measured using arsenazo III. *J. Neurosci.* **7**:3230–3244 (1987).
26. Sather, W., J. W. Johnson, G. Henderson, and P. Ascher. Glycine-insensitive desensitization of NMDA responses in cultured mouse embryonic neurons. *Neuron* **4**:725–731 (1990).
27. Jahr, C. E., and C. F. Stevens. Glutamate activates multiple single channel conductances in hippocampal neurons. *Nature (Lond.)* **325**:522–525 (1987).
28. Cull-Candy, S. G., and M. M. Usowicz. Multiple-conductance channels activated by excitatory amino acids in cerebellar neurons. *Nature (Lond.)* **325**:525–528 (1987).
29. Neher, E. The charge carried by single-channel currents of rat cultured muscle cells in the presence of local anaesthetics. *J. Physiol. (Lond.)* **339**:663–678 (1983).
30. Johnson, J. W., and P. Ascher. Glycine potentiates the NMDA response of mouse central neurones. *Nature (Lond.)* **325**:529–531 (1987).
31. Kleckner, N. W., and R. Dingledine. Requirement for glycine in activation of NMDA-receptors expressed in *Xenopus* oocytes. *Science (Washington D. C.)* **241**:835–837 (1988).
32. Lodge, D., and K. M. Johnson. Noncompetitive excitatory amino acid receptor antagonists. *Trends Pharmacol.* **11**:81–86 (1990).
33. Henderson, G., J. W. Johnson, and P. Ascher. Competitive antagonists and partial agonists at the glycine modulatory site of the mouse *N*-methyl-D-aspartate receptor. *J. Physiol. (Lond.)* **430**:189–212 (1990).
34. Carter, C. J., K. G. Lloyd, B. Zivkovic, and B. Scatton. Ifenprodil and SL 82.0715 as cerebral antiischemic agents. III. Evidence for antagonistic effects at the polyamine modulatory site within the *N*-methyl-D-aspartate receptor complex. *J. Pharmacol. Exp. Ther.* **253**:475–482 (1990).
35. Lester, R. A., M. L. Quarum, J. D. Parker, E. Weber, and C. E. Jahr. Interaction of 6-cyano-7-nitroquinoxaline-2,3-dione with the *N*-methyl-D-aspartate receptor-associated glycine binding site. *Mol. Pharmacol.* **35**:565–570 (1989).
36. Benveniste, M., J. Clements, L. Vyklicky, Jr., and M. L. Mayer. A kinetic analysis of the modulation of *N*-methyl-D-aspartic acid receptors by glycine in mouse cultured hippocampal neurones. *J. Physiol. (Lond.)* **428**:333–357 (1990).
37. Ransom, R. W. Ifenprodil inhibition of [^{3}H]glycine binding to the NMDA receptor: interactions with polyamines. *Soc. Neurosci. Abstr.* **16**:1042 (1990).
38. Skilling, S. R., D. H. Smullin, A. J. Beitz, and A. A. Larson. Extracellular amino acid concentrations in the dorsal spinal cord of freely moving rats following veratridine and nociceptive stimulation. *J. Neurochem.* **51**:127–132 (1988).
39. MacDonald, J. F., Z. Miljkovic, and P. Pennefather. Use-dependent block of excitatory amino acid currents in cultured neurons by ketamine. *J. Neurophysiol.* **58**:251–266 (1987).
40. Mayer, M. L., G. L. Westbrook, and L. Vyklicky, Jr. Sites of antagonist action on *N*-methyl-D-aspartic acid receptors studied using fluctuation analysis and a rapid perfusion technique. *J. Neurophysiol.* **60**:645–663 (1988).
41. Ascher, P., and L. Nowak. The role of divalent cations in the *N*-methyl-D-aspartate responses of mouse central neurones in culture. *J. Physiol. (Lond.)* **399**:247–266 (1988).
42. Williams, K., C. Romano, and P. B. Molinoff. Effects of polyamines on the binding of [^{3}H]MK-801 to the *N*-methyl-D-aspartate receptor: pharmacological evidence for the existence of a polyamine recognition site. *Mol. Pharmacol.* **36**:575–581 (1989).
43. Williams, K., V. L. Dawson, C. Romano, M. A. Dichter, and P. B. Molinoff. Characterization of polyamines having agonist, antagonist, and inverse agonist effects at the polyamine recognition site of the NMDA receptor. *Neuron* **5**:199–208 (1990).
44. Ransom, R. W., and N. L. Deschenes. Polyamines regulate glycine interaction with the *N*-methyl-D-aspartate receptor. *Synapse* **5**:294–298 (1990).
45. Shaw, G. G. The polyamines in the central nervous system. Biochem. Pharmacol. **28**:1–6 (1979).
46. Reynolds, I. J. Mechanisms underlying the interaction of polyamines with the NMDA receptor. *Soc. Neurosci. Abstr.* **16**:541 (1990).
47. Zorumski, C. F., J. Yang, and G. D. Fischbach. Calcium-dependent, slow desensitization distinguishes different types of glutamate receptors. *Cell. Mol. Neurobiol.* **9**:95–104 (1989).
48. MacDonald, J. F., I. Mody, and M. W. Salter. Regulation of *N*-methyl-D-aspartate receptors revealed by intracellular dialysis of murine neurones in culture. *J. Physiol. (Lond.)* **414**:17–34 (1989).
49. Elmslie, K. S., W. Zhou, and S. W. Jones. LHRH and GTP-γ-S modify calcium current activation in bullfrog sympathetic neurons. *Neuron* **5**:75–80 (1990).

Send reprint requests to: Gary L. Westbrook, Vollum Institute, L474, Oregon Health Sciences University, 3181 SW Sam Jackson Park Rd., Portland, OR 97201.